JOURNAL OF SOLID STATE CHEMISTRY 105, 279–286 (1993)

Synthesis, Crystal Structure, and Magnetic Susceptibilities of $CsFeP_2O_7$ and $RbFeP_2O_7$

EDITA DVONCOVA AND KWANG-HWA LII*

Institute of Chemistry, Academia Sinica, Taipei, Taiwan, Republic of China

Received July 27, 1992; in revised form November 3, 1992; accepted November 11, 1992

Two new ternary iron(III) diphosphates, $CsFeP_2O_7$ and $RbFeP_2O_7$, have been prepared and the structure of the Cs compound was determined from single-crystal X-ray diffraction data. Base on powder X-ray diffraction $RbFeP_2O_7$ adopts the same structure type as that of the Cs compound. $CsFeP_2O_7$ crystallizes in the monoclinic space group $P2_1/c$ with $a = 7.684(3)$, $b = 9.937(3)$, $c = 8.378(3)$ Å, $\beta = 104.84(3)°$, $V = 618.4(4)$ Å^3, $Z = 4$, and $R = 0.048$. The structure consists of intersecting tunnels running along the [001] and [110] directions, and the Cs^+ cations are located at the intersection of these tunnels. The framework is built up from corner-sharing FeO_6 octahedra and P_2O_7 groups. $CsFeP_2O_7$ is isostructural with $KFeP_2O_7$. Variable-temperature powder magnetic susceptibility data exhibit an antiferromagnetic transition at $T_N \sim 25$ K.

Introduction

Diphosphates of trivalent transition metals of the stoichiometry $A^IM^{III}P_2O_7$ (A = alkali metal, M = V, Fe, Mo) exhibit several structure types. The frameworks of these phases are built up from corner-sharing MO_6 octahedra and P_2O_7 groups. The size of the alkali metal cation plays an important role in the crystal structures of AMP_2O_7. The diphosphate group is very adaptive to the bonding requirements of other groups in the structures by adjusting the P–O–P bond angle and configuration of two phosphate tetrahedra. The lithium compounds $LiVP_2O_7$ (*1*), $LiFeP_2O_7$ (*2*), and $LiMoP_2O_7$ (*3*) are isostructural. $NaVP_2O_7$ (*4*) and $NaMoP_2O_7$ (*5*) are isostructural to the high-temperature form of the iron compound II-$NaFeP_2O_7$ (*6*). The low-temperature form, I-$NaFeP_2O_7$ (*7*), AMP_2O_7 (A = Cs, Rb, K; M = V, Mo) (*8*), and $KFeP_2O_7$ (*9*) are isostructural. To our knowledge, the two compounds that remain in this family, $CsFeP_2O_7$ and $RbFeP_2O_7$, have not been reported. In this work, we present the synthesis, single-crystal X-ray structure, and magnetic susceptibilities of $CsFeP_2O_7$, which is isostructural to $KFeP_2O_7$. Based on powder X-ray diffraction $RbFeP_2O_7$ adopts the same structure type as that of the Cs compound.

Experimental

Synthesis

Pink crystals of $CsFeP_2O_7$ were prepared by hydrothermal reaction of $CsOH_{(aq)}$ and $FePO_4$ (molar ratio Cs : Fe = 2 : 1) in 3.5 M $H_3PO_{4(aq)}$ in a sealed silica tube. The degree of fill in the glass tube was found to be 44%, including the volume of undissolved solid. The pressure inside the glass tube was balanced by an external pressure to keep the tube intact. The reaction was initially conducted at 500°C for 2d and yielded pink crystals which were too small to be used for single-crystal X-ray diffraction study. Subsequently, the same reaction tube was

* To whom correspondence should be addressed.

0022-4596/93 $5.00

heated at 550°C for 2*d* followed by slow cooling at 2°C/hr to 450°C. The reaction products contained large pink crystals of $CsFeP_2O_7$ of good quality, black crystals of $Fe_7(PO_4)_6$ (*10*), and unidentified white powder. Energy dispersive X-ray fluorescence analysis on a pink crystal showed that the Cs : Fe : P mole ratio was 1 : 1.04 : 2.15.

Based on powder X-ray diffraction, it was possible to prepare single-phase, polycrystalline $CsFeP_2O_7$ by heating a pressed pellet containing stoichiometric amounts of Cs_2CO_3, Fe_2O_3, and $(NH_4)_2HPO_4$ in air, first at 600°C for 4 hr to eliminate CO_2, H_2O, and NH_3, and then at 750°C for a week with several intermediate grindings. The product appeared air-stable in the laboratory atmosphere for at least a few days and was checked by powder X-ray diffraction. Attempts to grow crystals of $CsFeP_2O_7$ by solid-state reaction were unsuccessful.

Single phase polycrystalline $RbFeP_2O_7$ was obtained by heating a reaction mixture of $RbOH_{(aq)}$ and $FePO_4$ (molar ratio 2 : 1) in 3.5 *M* $H_3PO_{4(aq)}$ under the same hydrothermal conditions. X-ray powder patterns of $RbFeP_2O_7$ are shown over the 2θ range from 10 to 60° in Fig. 1. The observed pattern shown in (a) was recorded at room temperature with a Rigaku powder diffractometer and filtered Cu$K\alpha$ radiation. Shown in (b) is the calculated pattern obtained by using the unit cell parameters $a = 7.58$, $b = 9.97$, $c = 8.38$ Å and $\beta = 104.8°$, and assuming that the atomic coordinates for $RbFeP_2O_7$ are the same as those for $CsFeP_2O_7$.

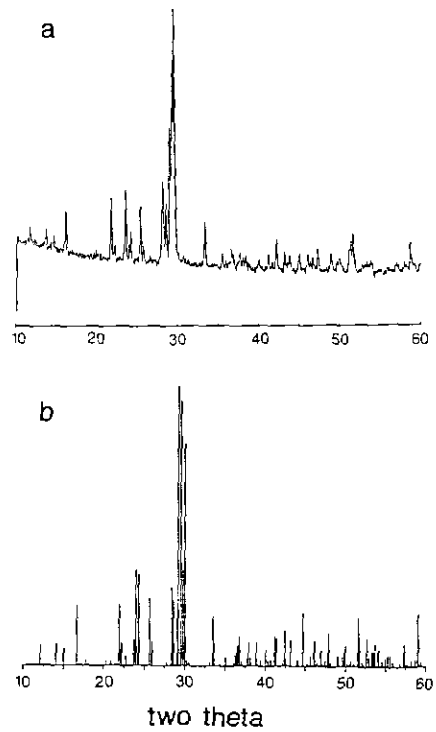

FIG. 1. Observed (a) and calculated (b) X-ray powder diffraction patterns of $RbFeP_2O_7$.

Single-Crystal X-Ray Diffraction

A pink crystal of $CsFeP_2O_7$ of approximate dimensions 0.5 × 0.5 × 0.4 mm was selected for indexing and intensity data collection on a Nicolet R3m/V four-circle diffractometer using graphite-monochromated Mo$K\alpha$ radiation. Unit cell parameters and orientation matrix were determined by a least-squares fit of 22 peak maxima with 2θ values ranging from 13 to 25°. Axial oscillation photographs were taken to check the symmetry properties and unit cell parameters. The intensity data were corrected for Lp and absorption effects. Correction for absorption effects were based on ψ scans of a few suitable reflections with χ values close to 90° using the program XEMP of the SHELXTL PLUS program package (*11*). On the basis of systematic absences, the space group was uniquely determined to be $P2_1/c$. The structure was solved by direct methods and successive Fourier synthesis, and were refined by full-matrix least-squares refinement based on *F* values. The multiplicity of the Cs atom was allowed to vary but did not deviate significantly from full occupancy. Therefore, the alkali metal site was considered fully occupied in subsequent calculations. The oxygen atoms were refined with isotropic thermal parameters since most of them gave nonpositive definite values when they were refined with anisotropic thermal parameters. This could be due to inadequate correction of absorption effect of the large crystal. The final cycle of

TABLE I

CRYSTAL DATA, INTENSITY MEASUREMENTS, AND REFINEMENT PARAMETERS FOR $CsFeP_2O_7$

1. Crystal data	
Crystal system	Monoclinic
Space group	$P2_1/c$
Cell constants	a = 7.684(3), b = 9.937(3), c = 8.378(3) Å, β = 104.84(3)°, V = 618.4(4) Å^3
Z	4
Density	3.896 g/cm^3
Abs. coeff. (Mo$K\alpha$)	86.98 cm^{-1}, $T_{min,max}$ = 0.489, 0.942
2. Intensity measurements	
λ(Mo$K\alpha$)	0.71073 Å
Scan mole	$\omega/2\theta$
Scan rate	3.01 – 14.65°/min in ω
Scan width	1.00° plus $K\alpha$ separation
Maximum 2θ	55°
Standard reflections	3 every 50 reflections (no decay)
Reflections collected	1718
3. Structure solution and refinement	
Unique reflections	1380 ($I > 3\sigma(I)$)
Parameters refined	66
Agreement factors[a]	R = 0.048, R_w = 0.059
GOF	1.32
$(\Delta\rho)_{max}$	2.37 e/Å^3 (at a distance of 0.5 Å from Cs)

[a] $R = \Sigma||F_o| - |F_c||/\Sigma|F_o|$; $R_w = [\Sigma w(|F_o| - |F_c|)^2/\Sigma w|F_o|^2]^{1/2}$.

least-squares refinement including the atomic coordinates, anisotropic thermal parameters for the Cs, Fe and P atoms, and isotropic thermal parameters for the O atoms converged at R = 0.048 and R_w = 0.059. All calculations were performed on a MicroVax II computer using SHELXTL Plus programs. Corrections for anomalous dispersion and secondary extinction were applied. Neutral atom scattering factors for all atoms were used. The crystallographic data are listed in Table I.

Magnetic Measurements

Magnetization data were obtained from 5 to 300 K in a magnetic field of 3 kG after zero field cooling using a SQUID magnetometer on 172.34 mg of polycrystalline sample. Both the zero field cooled and field cooled susceptibilities were measured. Observed susceptibilities were corrected for diamagnetism according to Selwood (*12*).

Results and Discussion

Final atomic coordinates and thermal parameters for $CsFeP_2O_7$ are listed in Table II. Selected bond distances, bond angles, and bond valence sums (*13*) are given in Table III. Bond valence sums for Fe and P are in good accordance with their formal oxidation states. The coordination number of Cs is determined on the basis of the maximum gap in the Cs–O distances ranked in increasing order. The maximum cation–anion distance, L_{max}, according to Donnay and Allmann (*14*) is also considered. Therefore, the Cs^+ cation is coordinated by 10 oxygen atoms at distances ranging from 2.957 to 3.404 Å. The 11th Cs–O distance is 3.710 Å. The bond valence sum for Cs is significantly higher than 1+, indicative of tightly bound Cs atom.

$CsFeP_2O_7$ is isostructural with $KFeP_2O_7$, I-$NaFeP_2O_7$, and $A^IM^{III}P_2O_7$ (A = Cs, Rb, K; M = V, Mo). The host lattice of these

TABLE II

ATOMIC COORDINATES AND THERMAL PARAMETERS (Å² × 100) for $CsFeP_2O_7$

Atom	x	y	z	U_{eq} [a, b]
Cs	0.69824(4)	0.70757(3)	0.03699(4)	1.45(2)
Fe	0.2593(1)	0.60097(7)	0.24187(9)	0.34(3)
P(1)	0.3695(2)	0.5923(1)	0.6664(2)	0.40(4)
P(2)	-.0775(2)	0.3745(1)	0.1814(2)	0.38(4)
O(1)	0.5158(5)	0.5006(3)	0.7650(4)	0.70(7)
O(2)	0.4060(5)	0.7351(3)	0.7310(4)	0.69(7)
O(3)	0.3409(5)	0.5796(4)	0.4845(5)	1.02(7)
O(4)	0.1848(5)	0.5435(3)	0.7053(4)	0.76(6)
O(5)	-.1784(5)	0.3991(4)	0.0058(5)	0.98(7)
O(6)	0.1103(5)	0.4352(3)	0.2279(4)	0.69(6)
O(7)	-.0671(5)	0.2264(3)	0.2336(4)	0.68(7)

Anisotropic thermal parameters (Å² × 100)[c]

	U_{11}	U_{22}	U_{33}	U_{23}	U_{13}	U_{12}
Cs	1.02(3)	1.82(3)	1.11(3)	-0.565(9)	-0.46(2)	0.30(1)
Fe	0.22(4)	0.40(4)	0.28(4)	-0.02(2)	-0.17(3)	0.02(2)
P(1)	0.26(6)	0.60(6)	0.23(6)	0.06(4)	-0.15(5)	0.14(4)
P(2)	0.24(6)	0.50(6)	0.27(6)	0.05(4)	-0.18(4)	0.04(4)

[a]The oxygen atoms were refined with isotropic thermal parameters.

[b]U_{eq} is defined as one-third of the trace of the orthogonalized U_{ij} tensor.

[c]Anisotropic temperature factors are of the form: Temp = $\exp[-2\pi^2(h^2U_{11}a^{*2} + \cdots + 2hkU_{12}a^*b^* + \cdots)]$.

compounds $[M^{III}P_2O_7]$ is built up from corner-sharing MO_6 octahedra and P_2O_7 groups. Each MO_6 octahedron is linked to five different P_2O_7 groups, and each P_2O_7 group shares its six corners with five different MO_6 octahedra and is bonded to one of the MO_6 octahedra through bidentate bonding. The two PO_4 tetrahedra of a P_2O_7 group are in a staggered configuration. The P–O bond distances in two independent PO_4 tetrahedra in $CsFeP_2O_7$ can be divided into three groups: one long distance at 1.610 and 1.627 Å corresponding to the P–O–P bond, two intermediate distances at 1.516–1.519 and 1.520–1.532 Å, and one short distance at 1.489 and 1.497 Å. Most of the O atoms which are involved in the intermediate P–O bonds are bonded to two Cs atoms instead of one for those in the short bonds. The distortion of a PO_4 tetrahedron can be estimated by using the equation $\Delta = (\frac{1}{4})\Sigma((R_i - \bar{R})/\bar{R})^2$ where R_i = an individual bond length and $\bar{R}$ = average bond length (*15*). The calculation results indicate that the PO_4 tetrahedra in $CsFeP_2O_7$ are slightly more distorted than those in $KFeP_2O_7$. The

TABLE III

BOND LENGTHS (Å), BOND ANGLES (°), AND BOND VALENCE SUMS (Σs) FOR $CsFeP_2O_7$

		Bond lengths	
Cs-O(1)a	3.122(3)	Cs-O(1)b	3.337(4)
Cs-O(2)a	2.957(3)	Cs-O(2)c	3.143(4)
Cs-O(3)c	3.404(4)	Cs-O(4)b	3.271(4)
Cs-O(5)d	3.239(4)	Cs-O(6)e	3.282(4)
Cs-O(6)f	3.111(3)	Cs-O(7)f	2.995(4)
Σs(Cs-O) = 1.34			
Fe-O(1)b	2.015(4)	Fe-O(2)c	1.996(4)
Fe-O(3)	1.979(4)	Fe-O(5)g	2.008(4)
Fe-O(6)	1.992(3)	Fe-O(7)h	1.983(4)
Σs(Fe-O) = 3.17			
P(1)-O(1)	1.516(4)	P(1)-O(2)	1.519(4)
P(1)-O(3)	1.489(4)	P(1)-O(4)	1.610(4)
Σs(P(1)-O) = 5.05			
P(2)-O(5)	1.497(4)	P(2)-O(6)	1.520(4)
P(2)-O(7)	1.532(4)	P(2)-O(4)i	1.627(4)
Σs(P(2)-O) = 4.91			
		Bond angles	
O(3)-Fe-O(6)	89.9(1)	O(3)-Fe-O(1)b	85.8(2)
O(3)-Fe-O(2)c	95.8(1)	O(3)-Fe-O(5)g	173.8(2)
O(3)-Fe-O(7)h	90.5(2)	O(6)-Fe-O(1)b	93.9(1)
O(6)-Fe-O(2)c	174.1(2)	O(6)-Fe-O(5)g	85.3(1)
O(6)-Fe-O(7)h	95.4(2)	O(1)b-Fe-O(2)c	84.8(2)
O(1)b-Fe-O(5)g	90.6(2)	O(1)b-Fe-O(7)h	170.0(1)
O(2)c-Fe-O(5)g	89.0(1)	O(2)c-Fe-O(7)h	86.3(2)
O(5)g-Fe-O(7)h	93.8(2)	O(1)-P(1)-O(2)	108.9(2)
O(1)-P(1)-O(3)	113.7(2)	O(1)-P(1)-O(4)	106.1(2)
O(2)-P(1)-O(3)	114.1(2)	O(2)-P(1)-O(4)	107.5(2)
O(3)-P(1)-O(4)	106.0(2)	O(5)-P(2)-O(6)	114.0(2)
O(5)-P(2)-O(7)	114.4(2)	O(5)-P(2)-O(4)i	106.2(2)
O(6)-P(2)-O(7)	109.4(2)	O(6)-P(2)-O(4)i	104.0(2)
O(7)-P(2)-O(4)i	108.2(2)		

Note. Symmetry codes: (a) $x, y, -1 + z$; (b) $1 - x, 1 - y, 1 - z$; (c) $x, 1.5 - y, -0.5 + z$; (d) $1 + x, y, z$; (e) $1 - x, 1 - y, -z$; (f) $1 - x, 0.5 + y, 0.5 - z$; (g) $-x, 1 - y, -z$; (h) $-x, 1 - y, 0.5 - z$; (i) $-x, 1 - y, 1 - z$.

P–O–P bond angle involving the bridging oxygen in $CsFeP_2O_7$ (124.9°) is about the same as that in the K compound (124.3°) The FeO_6 octahedra in $CsFeP_2O_7$ are almost regular as shown by the Fe–O distances and O–Fe–O bond angles, and the octahedral distortion is less than that in $KFeP_2O_7$.

The structure of $CsFeP_2O_7$ can be regarded as resulting from stacking along [001] of $[FeP_2O_7]_\infty$ layers parallel to the (001)

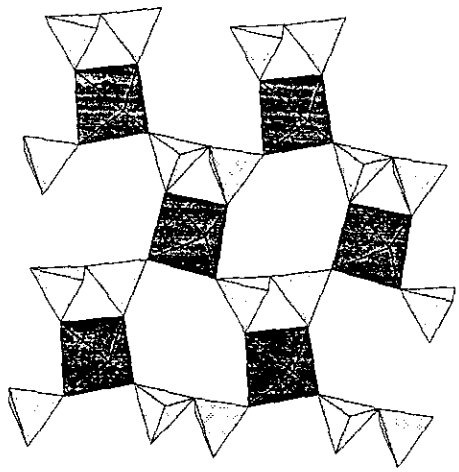

FIG. 2. View along the [001] direction of a $[FeP_2O_7]_\infty$ layer in $CsFeP_2O_7$.

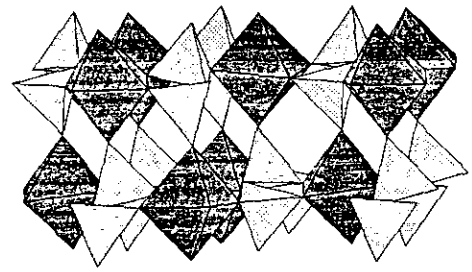

FIG. 3. View along [100] showing the connection between two $[FeP_2O_7]_\infty$ layers in $CsFeP_2O_7$.

plane. Each layer shows heptagonal windows formed by the edges of three octahedra and four tetrahedra (Fig. 2). Adjacent layers are generated by the *c*-glide planes to form a three-dimensional network with tunnels running along the *c*-axis (Figs. 3 and 4). The connectivity of the P_2O_7 groups to the FeO_6 octahedra is interesting. The height of a P_2O_7 corresponds to that of an octahedron, and one P_2O_7 group alternates with an octahedron, thus forming a double chain parallel to the *c*-axis (Fig. 5). Along the [110] direction one also observes hexagonal tunnels formed by the edges of two octahedra and four tetrahedra, and small tetragonal tunnels of two octahedra and two tetrahedra (Fig. 6). The Cs^+ cations are situated at the intersection of these tunnels with tenfold coordination (Fig. 7). The coordination environment of the Cs^+ ion is essentially the same as that of the K^+ ion in $KFeP_2O_7$ except that the K–O bond lengths are shorter.

As shown in Fig. 8, the variation of reciprocal molar susceptibility $1/\chi_M$ versus temperature shows a minimum at ~25 K which is very likely due to antiferromagnetic tran-

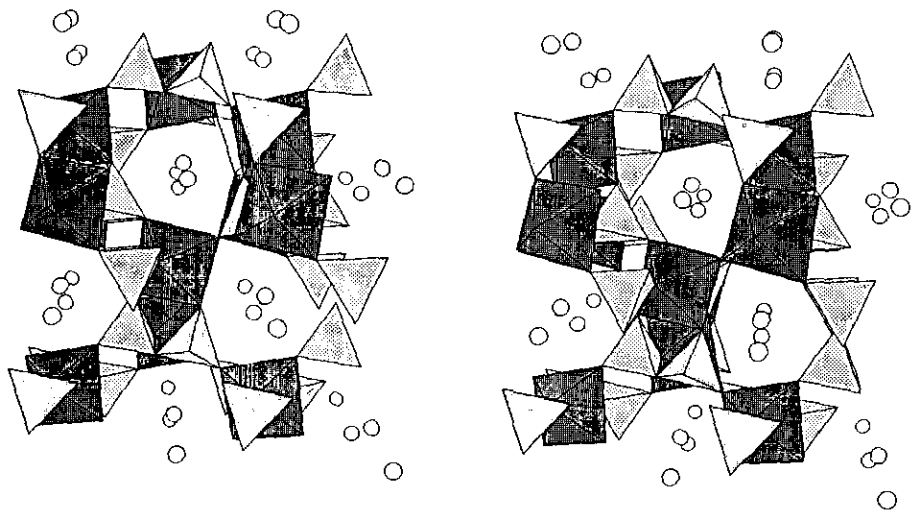

FIG. 4. Stereoscopic view of the $CsFeP_2O_7$ structure along [001].

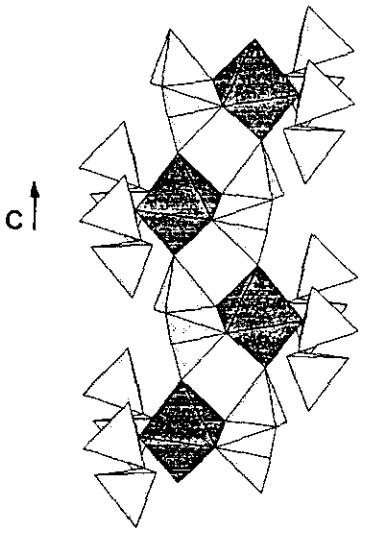

FIG. 5. The coordination of P_2O_7 ligands around FeO_6 octahedra in $CsFeP_2O_7$. The view is perpendicular to the tunnel direction.

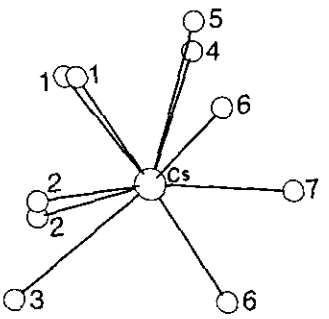

FIG. 7. Projection along [001] showing the environment of the Cs^+ ion.

sition. The magnetic data between 50 and 300 K are described very well by a Curie–Weiss behavior: $\chi_M = C/(T - \theta)$, where $C = 3.86$ cm$^3 \cdot$ K/mole and $\theta = -64.9$ K. If the Weiss temperature θ is corrected for the Weiss field, the effective magnetic moment is ca. 5.6 μ_B and essentially independent of temperature above 50 K. The moment is a little lower than the spin-only value of high-spin Fe^{3+} (5.9 μ_B). The magnetic susceptibilities of $AFeP_2O_7$ (A = Li, Na, K) reported by Riou *et al.* (*16*) exhibit an antiferromagnetic transition at $T_N \sim 20$ K. The Weiss constant decreases from $NaFeP_2O_7$ (-58 K) to $KFeP_2O_7$ (-90 K) via $LiFeP_2O_7$ (-73 K) while the mean Fe–Fe distance increases from 5.615 to 5.641 Å and the number of nearest Fe^{3+} ions surrounding one iron cation decreases. The difference in the Weiss constants was explained on the basis of the Fe–Fe distance and the number of neighboring Fe^{3+} ions. In $CsFeP_2O_7$ each iron cation is surrounded by 10 Fe^{3+} ions at distances ranging from 5.11 to 6.47 Å with an average value of 5.76 Å. The Weiss constant for $CsFeP_2O_7$ can not be explained by the same argument.

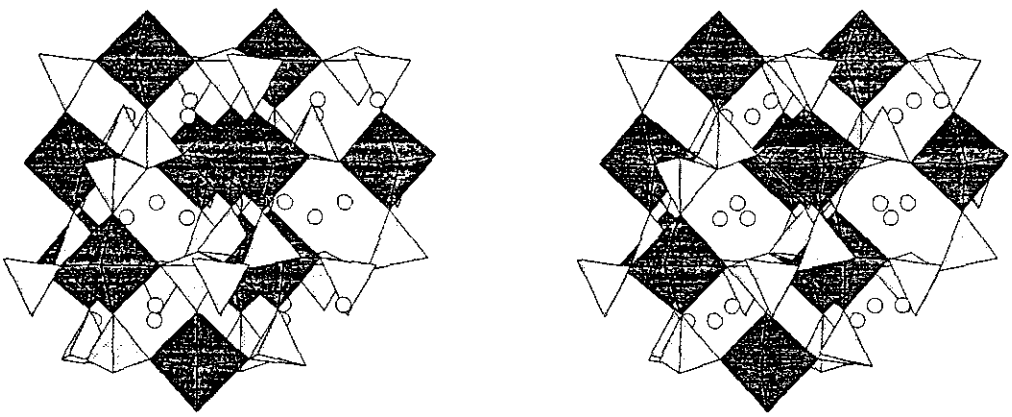

FIG. 6. Stereoscopic view of the $CsFeP_2O_7$ structure in a direction approximately along [110].

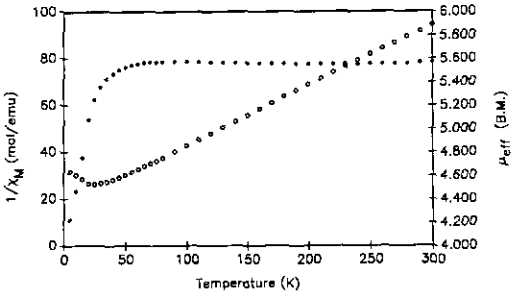

FIG. 8. A plot of inverse molar magnetic susceptibility (open circle) and the effective magnetic moment (solid circle) of $CsFeP_2O_7$ as a function of temperature. The moment is calculated from the equation $\mu_{eff} = 2.83[\chi_M(T - \theta)]^{1/2}$ where θ is -64.9 K.

Acknowledgments

Support for this study by the National Science Council and the Institute of Chemistry Academia Sinica is gratefully acknowledged. We thank Professor Sue-Lein Wang at the Department of Chemistry, National Tsing Hua University for X-ray intensity data collection.

References

1. K. H. LII, Y. P. WANG, Y. B. CHEN, AND S. L. WANG, *J. Solid State Chem.* **86,** 143 (1990).
2. E. A. GENKINA, B. A. MAKSIMOV, V. A. TIMOFEEVA, A. B. BYKOV, AND O. K. MEL'NIKOV, *Sov. Phys. Dokl.* **30,** 817 (1985).
3. S. L. WANG, P. C. WANG, AND Y. P. NIEH, *J. Appl. Crystallogr.* **23,** 520 (1990).
4. Y. P. WANG, K. H. LII, AND S. L. WANG, *Acta Crystallogr. Sect. C* **45,** 673 (1989).
5. A. LECLAIRE, M. M. BOREL, A. GRANDIN, AND B. RAVEAU, *J. Solid State Chem.* **76,** 131 (1988).
6. M. GABELICA-ROBERT, M. GOREAUD, PH. LABBE, AND B. RAVEAU, *J. Solid State Chem.* **45,** 389 (1982).
7. J. P. GAMONDES, F. D'YVOIRE, AND A. BOULLE, *C. R. Acad. Sci. Paris Ser. C* **269,** 1532 (1969).
8. $CsVP_2O_7$: Y. P. WANG AND K. H. LII, *Acta Crystallogr. Sect. C* **45,** 1210 (1989); $RbVP_2O_7$: K. H. Lii, unpublished research; KVP_2O_7: L. Benhamada, A. Grandin, M. M. Borel, A. Leclaire, and B. Raveau, *Acta Crystllogr. Sect. C* **47,** 424 (1991); $CsMoP_2O_7$: K. H. Lii and R. C. Haushalter, *Acta Crystallogr. Sect. C* **43,** 2036 (1987); $RbMoP_2O_7$: D. Riou, A. Leclaire, A. Grandin, and B. Raveau, *Acta Crystallogr. Sect. C* **45,** 989 (1989); $KMoP_2O_7$: J. J. Chen, C. C. Wang, and K. H. Lii, *Acta Crystallogr. Sect. C* **45,** 673 (1989) and A. Leclaire, M. M. Borel, A. Grandin, and B. Raveau, *J. Solid State Chem.* **78,** 220 (1989).
9. D. RIOU, PH. LABBE, AND M. GOREAUD, *Eur. J. Solid State Inorg. Chem.* **25,** 215 (1988).
10. YU. A. GORBUNOV, B. A. MAKSIMOV, YU. K. KABALOV, A. N. IVASHCHENKO, O. K. MEL'NIKOV, AND N. V. BELOW, *Dokl. Akad. Nauk SSSR* **254,** 873 (1980).
11. G. M. SHELDRICK, SHELXTL-PLUS Crystallographic System, release 4.11. Siemens Analytical X-Ray Instruments, Inc., Madison, WI (1990).
12. P. W. SELWOOD, "Magnetochemistry," Interscience, New York (1956).
13. I. D. BROWN AND D. ALTERMATT, *Acta Crystallogr. Sect. B* **41,** 244 (1985).
14. G. DONNAY AND R. ALLMAN, *Am. Mineral.* **55,** 1003 (1970).
15. R. D. SHANNON, *Acta Crystallogr. Sect. A* **32,** 751 (1976).
16. D. RIOU, N. NGUYEN, R. BENLOUCIF, AND B. RAVEAU, *Mater. Res. Bull.* **25,** 1363 (1990).